Evaluation of Weather Parameters for Renewable Energy Forecasting with Echo State Networks

Samuel G. Dotson[a],[*], Kathryn D. Huff[a]

[a]*Dept. of Nuclear, Plasma, and Radiological Engineering, University of Illinois at Urbana-Champaign, Urbana, IL 61801*

Abstract

Calls for decarbonization have led to rapid growth of solar photovoltaic cells and wind turbines. These energy sources vary based on weather features such as solar irradiance and wind speed. This variability challenges grid operators to reliably meet demand through scheduling dispatchable resources. This paper uses weather and energy data from the diverse microgrid at the University of Illinois at Urbana-Champaign to develop accurate forecasts for total electricity demand, wind power, and solar power with echo state networks. We found that solar elevation angle was the only parameter that improved the forecast in every case. Other parameters must be chosen carefully for each application.

Keywords: renewable energy, forecasting, machine learning, echo state networks, grid planning

1. Introduction

1.1. Motivation

In response to the rising threat of climate change, many countries have prioritized reducing carbon emissions. The 2015 Paris Agreement aims to prevent the global temperature from rising more than 1.5 °C above pre-industrial levels [1]. Virtually all current plans to reduce carbon emissions depend on increasing the share of energy production by renewable and clean energy sources,

---

[*]Corresponding Author

Email address: `sgd2@illinois.edu` (Samuel G. Dotson)

especially solar and wind [2, 3, 4, 5]. While solar and wind generate zero carbon emissions, these forms of electricity generation increase grid variability, which can lead to blackouts and power system failures [6]. Further, even modest variable energy penetration negatively affects the economics of other clean energy sources, such as nuclear power [2, 7, 8]. This may force nuclear plants to shut down prematurely, at the precise moment that all clean sources of energy are most needed. Some existing work quantified the economic benefit of improving renewable energy forecasts [9, 10, 11]. Improving renewable energy forecasts can mitigate some of the negative side effects of variability. The economic benefits of better forecasts include: reduced costs compared to building storage devices [9]; curtailment reduction and more efficient use of non-renewable sources [10]; and modest load-following from nuclear and biomass generators, which are unable to follow rapid changes in demand [11]. Most proposed forecasting improvements involve new algorithms or machine learning techniques. However, one of the simplest approaches to improving forecasts is to improve the training data for such algorithms. There is a veritable zoo of weather parameters that can supplement target training data, but we don't know *a priori* which of these parameters will be helpful or detrimental to model performance. In this paper, we evaluate several common parameters for use in renewable energy forecasting with Echo State Networks (ESNs).

1.2. Why Echo State Networks

ESNs have several appealing features. Simplicity, consisting only of a large, sparse, reservoir and a single output layer [12]; flexibility and generalizability, while other network architectures require significant fine tuning [13]; and speed, due to their simple structure and few trainable weights relative to other neural networks. The ESN network architecture eliminates the need for complicated data pre-processing, such as feature extraction, that is required for other machine learning and statistical algorithms [14, 15]. ESNs can also outperform other prediction techniques [16, 17, 18, 19, 20].

Classical ESNs have previously been used to forecast demand, wind energy,

2

and solar energy [21, 17, 20]. Typically, ESNs make extreme short term predictions, on the order of seconds or minutes [22, 23, 19], one-hour ahead [18], and up to one ahead [21]. Forecasts must be at least 4-hours ahead [9] to 48-hours ahead [9, 10, 11] to aid resource scheduling and grid-scale energy economy. In this work we use a classic ESN architecture to forecast total demand, wind production, and solar production, 4-hours and 48-hours ahead.

Approaches in the literature to improve the forecasting capability of the basic ESN include: adding multiple reservoirs [20, 24, 25, 26], including non-linear units [27, 19], combining with other network architecture [22, 28]; and using a particle swarm approach [29, 23]. Some work indicates that including weather parameters may be useful for renewable energy forecasting [30, 19], but none have demonstrated the effect each parameter has on model performance. The primary goal of this work is to fill that gap.

1.3. Contributions

In this work, we use ESNs to predict three key values: total electricity demand, wind energy production, and solar energy production. We split these tasks into further sub tasks, predicting 4-hours ahead and 48-hours ahead. These predictions facilitate scheduling and grid planning because current market rules put renewable energy on the grid first, forcing conventional power generators to work around this variability [9]. Using ESNs to make predictions two days ahead is unique to this paper since the longest predictions by ESNs in the literature only reach one day ahead [21]. Finally, we repeat these tasks with several commonly used weather parameters and evaluate their effect on model performance. The need to consider exogenous meteorological inputs has been noted in the literature [19]. Suprisingly, sun elevation is seldom used as a correlated quantity for energy demand and wind power.

In Section 2 of this paper, we discuss how data were selected and processed, and we review ESNs. Section 3 shows a benchmarking exercise for our ESN implementation and presents the results. We discuss the results and future implications in Section 4.

2. Methodology

2.1. Echo State Networks

An ESN, sometimes called a "reservoir computer,"[31, 32, 33] is a type of recurrent neural network [34] that replaces the many hidden layers of a conventional feed-forward neural network with a reservoir that is:

1. sparse,

2. connected by uniformly random weights, centered at zero,

3. and large (i.e. has many neurons).

The reservoir is therefore a randomly instantiated adjacency matrix, $\boldsymbol{W}$, of size $N \times N$. An input matrix W^{in}, of size $N \times K$, maps the input vector, $U(t)$ with K units, onto the reservoir. The activation states of the reservoir are calculated by [18, 32, 12]

$$x(t) = \tanh\left(W^{in} \cdot U(t) + \mathbf{W}x(t-1)\right) \tag{1}$$

where

$$x(t) = \text{the collection of reservoir activations.}$$

The output, $U(t + \Delta t)$, is read by an output weight matrix, W^{out}, thus:

$$U(t + \Delta t) = \left(W^{out}\right)^T \cdot x(t). \tag{2}$$

In the training phase, we discard the output and the next training input is passed to the network. During the prediction phase, we keep the output and use it as the next input. Figure 1 illustrates this behavior. The speed of ESNs is owed to this structure – only W^{out} has tunable weights. Everything else is fixed. In this work, we adapted the open source Python package `pyESN` [35] to construct and train the network.

4
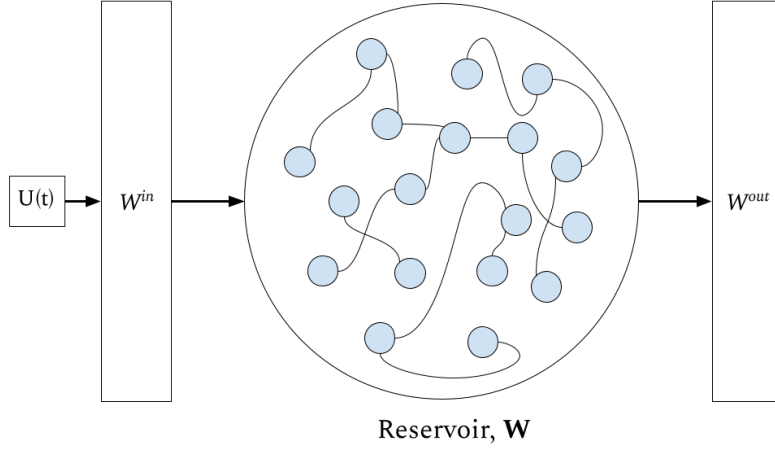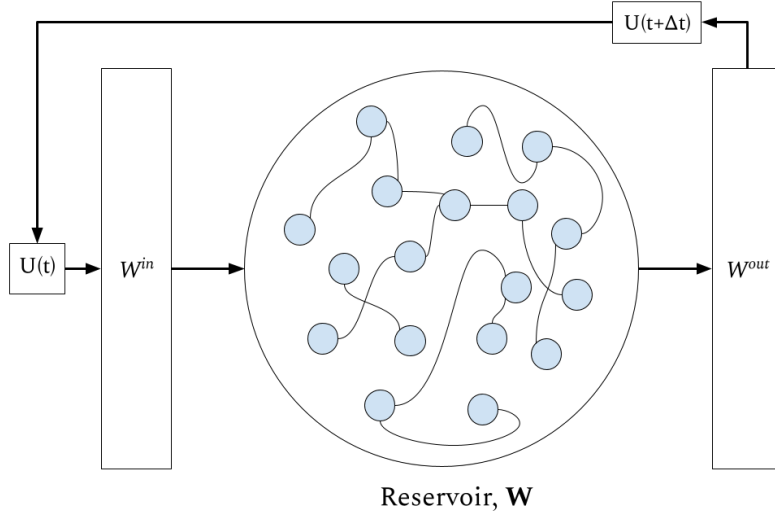
(a) Training Flow

(b) Predicting Flow

Figure 1: (a) Shows the behavior of an ESN during the training phase. (b) Shows ESN behavior during the predicting phase. The output $U(t + \Delta t)$ is used as the next input value.

2.2. Hyper-Parameter Optimization

ESNs are fast because a large reservoir, that does not require training, replaces the hidden layers in a conventional feed-forward neural network. The trade-off is that ESNs are sensitive to various hyper-parameters that must be optimized [12]. Table 1 summarizes these hyper-parameters. The spectral radius (ρ) should satisfy the "echo state property" which means that previous reservoir activations have a decaying influence on future states. This is usually guaranteed for $\rho < 1$, but is not a requirement [12]. We optimize the hyper-parameters by performing

Table 1: Description of Model Hyper-Parameters

Hyper-parameter	Purpose	Tested Values
`noise`	Neuron regularization	[0.0001, 0.0003, 0.0007, 0.001, 0.003, 0.005, 0.007, 0.01]
ρ	Spectral radius	[0.5, 0.7, 0.9, 1, 1.1, 1.2, 1.3, 1.5]
N	Size of reservoir, $\mathbf{W}$	[600, 800, 1000, 1500, 2000, 2500, 3000, 4000]
`sparsity`	The density of connections in $\mathbf{W}$	[0.005, 0.01, 0.03, 0.05, 0.1, 0.12, 0.15, 0.2]
Training Length	Training set size	$L \in [5000, 25000]$, step size $= 300$

a grid search over the test values specified in Table 1. We took the following optimization steps for each prediction task:

1. Select a hyper-parameter or pair of parameters.
2. Generate ESN prediction with the specified parameters.
3. Calculate and record the root mean squared error (RMSE).
4. Continue until last entry in the parameter set is reached.
5. Set the network parameters to hyper-parameter value that minimizes the RMSE.

Figure 2 shows an example heatmap that optimized the spectral radius and noise hyper-parameters for the 4-hour ahead demand forecast and illustrates the sensitivity of ESNs to hyperparameter values.
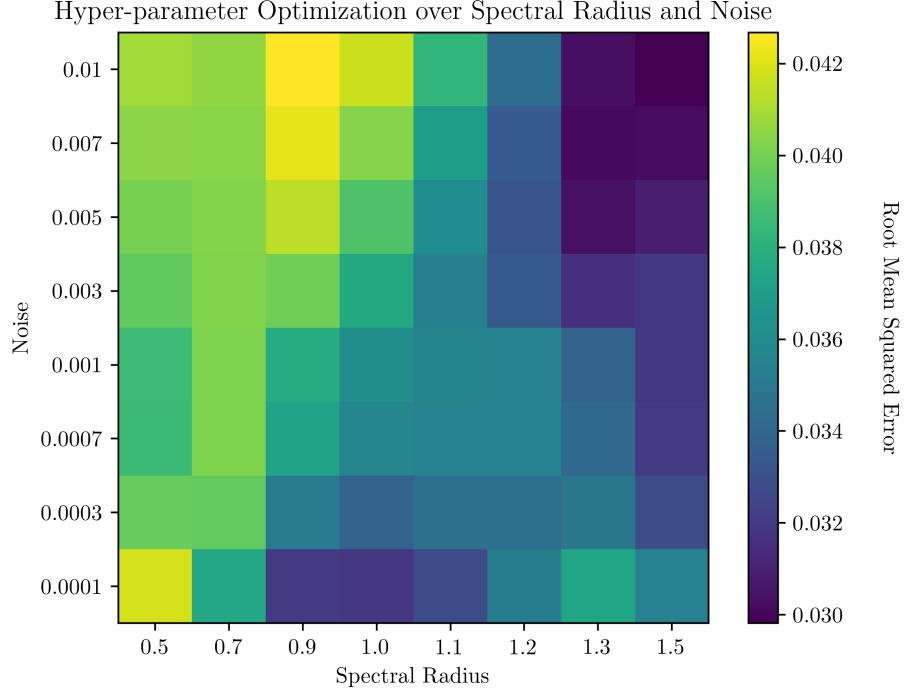
Figure 2: An example heatmap of the RMSE for 4-hour ahead demand prediction with different combinations of spectral radius, ρ, and noise.

2.3. Prediction Tasks

In order to verify that the performance of our ESN implementation was consistent with the literature [31] we first performed a benchmarking task by making a prediction for the Lorenz 1963 model. The Lorenz 1963 model is described by a system of coupled differential equations:

$$\frac{\mathrm{d}x}{\mathrm{d}t} = \sigma(y - x), \tag{3}$$

$$\frac{\mathrm{d}y}{\mathrm{d}t} = x(\rho - z) - y, \tag{4}$$

$$\frac{\mathrm{d}z}{\mathrm{d}t} = xy - \beta z, \tag{5}$$

where

$$\sigma = 10,$$
$$\beta = 8/3,$$
$$\rho = 28,$$

since the system demonstrates chaotic behavior for these parameter values [36].

Next, we optimized predictions for univariate time-series representing total demand, solar energy, and wind energy 4-hours ahead and 48-hours ahead. Finally, we repeated those same six tasks with an additional predictor. One value from each column in Table 2 was selected for each task for a total of 42 predictions.

Table 2: Summary of prediction tasks.

Target	Future	Additional Predictor
		None
Total Demand		Solar Elevation
	4-hours ahead	Humidity
Solar Energy		Pressure
	48-hours ahead	Wet Bulb Temp.
Wind Energy		Dry Bulb Temp.
		Wind Speed

2.4. Data Selection and Processing

The University of Illinois at Urbana-Champaign (UIUC) Solar Farm 1.0 dashboard provides data for the solar energy generated on campus [37]. The UIUC Facilities and Services Department shared proprietary data for campus electricity demand and wind energy with us [38]. All data had hourly resolution. Weather data were retrieved from the National Oceanic and Atmospheric

Administration (NOAA)[39] for two locations: Champaign, IL, where UIUC is located, and Lincoln, IL, where Railsplitter Windfarm is located. UIUC has a power purchase agreement with Railsplitter Windfarm [40].

In the case of UIUC solar data, significant portions were missing due to instrument failure. In order to fill in this missing data, we calculated the theoretical solar energy production based on irradiance data from OpenEI [41, 42] with

$$P = G_T \eta_{ref} \tau_{pv} A \left(1 - \gamma \left(T - 25\right)\right) \ \left[W\right] \tag{6}$$

where

$$P = \text{ the total power of the solar farm}$$

$$G_T = \text{ the total incident solar irradiance}$$

$$= P_{DNI} \cos\left(\beta + \delta - lat\right) + P_{DHI} \left(\frac{180 - \beta}{180}\right) \left[\frac{W}{m^2}\right] \tag{7}$$

and

$$\delta = \text{ the solar declination angle}$$

$$= 23.44 \sin\left(\left(\frac{\pi}{180}\right)\left(\frac{360}{365}\right)(N + 284)\right) [°] \tag{8}$$

$$\eta_{ref} = \text{ conversion efficiency [-]}$$

$$\tau_{pv} = \text{ transmittance [-]}$$

$$\gamma = \text{ thermal coefficient [-]}$$

$$A = \text{ solar panel coverage } [m^2]$$

$$P_{DNI} = \text{direct normal irradiance } \left[\frac{W}{m^2}\right]$$

$$P_{DHI} = \text{diffuse horizontal irradiance } \left[\frac{W}{m^2}\right]$$

$$\beta = \text{tilt angle of the solar panels } [°]$$

We also calculated the solar elevation angle, α, using coordinates for the UIUC

Solar Farm 1.0 [43, 44],

$$\alpha = \sin^{-1}\left[\sin(\delta)\sin(\phi) + \cos(\delta)\cos(\phi)\cos(\omega)\right] [°] \tag{9}$$

where

$$\delta = \text{declination angle } [°]$$
$$\phi = \text{latitude of interest } [°]$$
$$\omega = \text{hour angle } [°]$$

Finally, we normalized all of the data using the infinity norm

$$\|\mathbf{x}\|_{\infty} \equiv \max |x_i|. \tag{10}$$

The infinity norm is equivalent to normalizing by the system capacity. This simplifies the comparison of our results between tasks whose training data have vastly different magnitudes. This normalization also makes it possible to compare results with other work and is consistent with the recommendation from Kobylinski et al. (2020) [45]. Table 3 gives the maximum value for each system.

Table 3: Description of the size of the UIUC microgrid

System	Maximum Value
Electricity Demand	81.6 [MW]
Solar Energy	4.7 [MW]
Wind Energy	8.8 [MW]

2.5. Performance Metrics

We measured the accuracy of the model using two error metrics: mean absolute error (MAE) and root mean squared error (RMSE). These are defined

as

$$\text{MAE} = \frac{1}{N} \sum_{i=1}^{N} |y_i - \hat{y}_i| \tag{11}$$

$$\text{RMSE} = \sqrt{\frac{1}{N} \sum_{i=1}^{N} (y_i - \hat{y}_i)^2} \tag{12}$$

where

$$\hat{y}_i = \text{predicted output}$$

$$y_i = \text{true value}$$

The MAE measures the expected error throughout the forecast horizon. The RMSE indicates the presence of significant but infrequent errors. Since the data were normalized by system capacity [9], the error metrics are easily interpretable. In order to compare how each individual weather input changed the forecast accuracy, we calculated a "percent improvement" over the univariate case (i.e. a demand prediction based only on historical demand data). This percent improvement, Δe, is calculated as

$$\Delta e = \frac{\hat{e} - e}{e} \times 100, \ [\%] \tag{13}$$

where

$$e = \text{error from the univariate forecast}$$

$$\hat{e} = \text{error from the duovariate forecast.}$$

The sign indicates the direction of change in error. Finally, in order to further facilitate comparison with other work, we calculated the normalized root mean squared error (NRMSE) by

$$NRMSE = \sqrt{\frac{\sum_{i=1}^{N} (y_i - \hat{y}_i)^2}{\sum_{i=1}^{N} (y_i - \tilde{y}_i)^2}} \tag{14}$$

where

$$\tilde{y} = \text{mean of the target set.}$$

11

3. Results

3.1. Benchmark: Lorenz 1963

We first verified that our choice of implementation for a conventional ESN produced similar results to those found in the literature [31]. Table 4 contains the hyper-parameters that minimized the RMSE of the model. Our optimized values differ somewhat from the literature, but our ESN implementation succesfully replicated the climate of the Lorenz Attractor similar to Pathak et. al 2017 [31]. Figure 3 shows the ESN forecast ten seconds into the future for the Lorenz 1963 model.

Table 4: Hyper-parameters for the ESN that predicted the Lorenz 1963 model. The random seed was generated by the open source packag `numpy`.

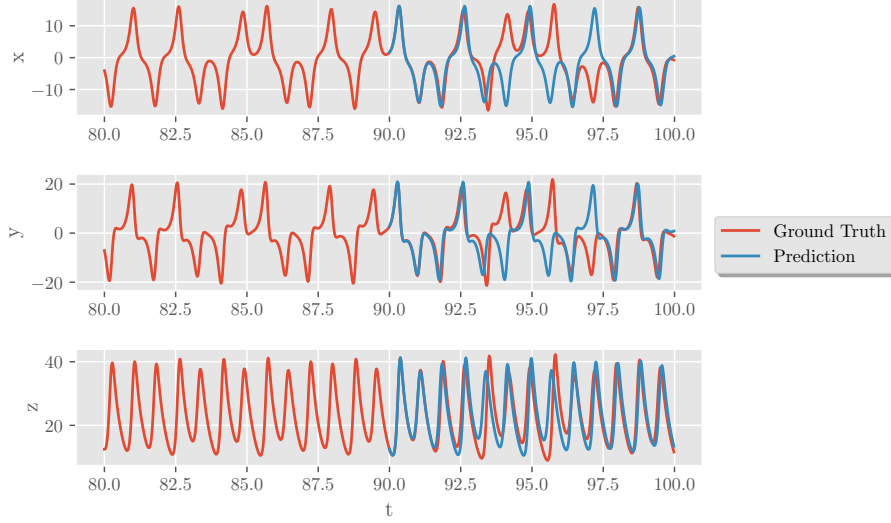| Parameter	This paper	Literature [31]
N	2000	300
ρ	0.9	1.2
`sparsity`	0.1	0.1
`noise`	0.001	0
Training Length	3200	Not Specified
Random Seed	85	Not Specified

Figure 3: Using an ESN to replicate the climate of the Lorenz Attractor.

3.2. ESN Forecasting: Demand

We used ESNs to forecast electricity demand, or electric load, at both 4-hour

¹³⁵ intervals and 48-hour intervals. Figure 4 shows the 48-hour ahead forecast that had the lowest RMSE. In this case, the forecast that used relative humidity as an additional input had the lowest error, as shown in Table 5. Table 5 also shows that the forecast was weakened by training with air temperature (both wet bulb and dry bulb), air pressure, and wind speed. Adding solar elevation

¹⁴⁰ angle performed approximately the same as the base case.

Figure 5 shows the 4-hour interval forecast with the lowest RMSE. Solar elevation angle improved the forecast more than any other meteorological input. Table 6 shows that humidity, air pressure, dry bulb temperature, and wind speed worsened the forecast.

¹⁴⁵ This implementation performance is consistent with previous applications of ESNs to the task of predicting electric load [21]. Further, these results indicate that ESNs perform better than other machine learning techniques, Long Short-Term Memory (LSTM) [46], Sequence to Sequence (S2S) [46], and support vector regression [15], for predicting energy demand.
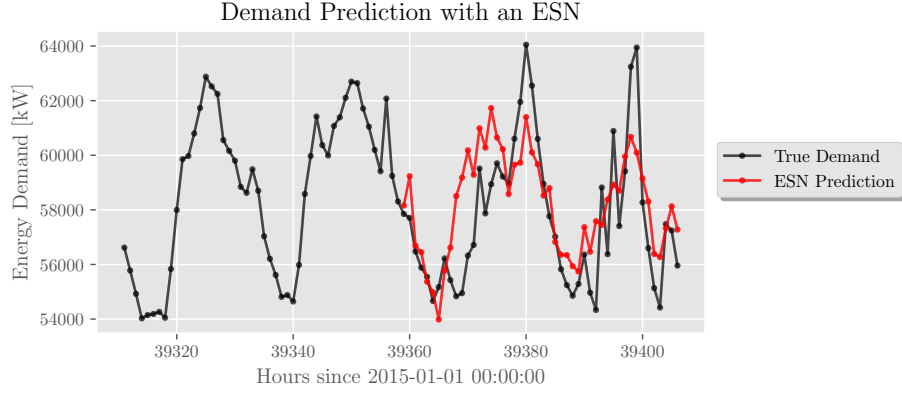
13

Figure 4: The optimized 48-hour ahead demand prediction. The training inputs for this forecast were historical hourly demand and relative humidity. *Hyperparameters*: Reservoir Size: 1500, Sparsity: 0.2, Spectral Radius: 1.5, Noise: 0.0007, Training Length: 5000, Prediction Window: 48, Random state: 85

Table 5: Tabulated error for 48-hour ahead electricity demand forecasts with various coupled quantities.

| Scenario	NRMSE	MAE	RMSE	Improvement MAE (%)	Improvement RMSE (%)
Total Demand	0.76691	0.0189	0.0241	[-]	[-]
Demand + Sun Elevation	0.76351	0.0191	0.0240	+1.0582	-0.4149
Demand + Humidity	0.70799	0.0180	0.0223	-4.7619	-7.4689
Demand + Pressure	0.77769	0.0176	0.0245	-6.8783	+1.6600
Demand + Wet Bulb Temp.	0.99886	0.0241	0.0314	+27.5132	+30.2904
Demand + Dry Bulb Temp.	0.86634	0.0218	0.0273	+15.3439	+13.2780
Demand + Wind Speed	0.77958	0.0197	0.0245	+4.2328	+1.6600
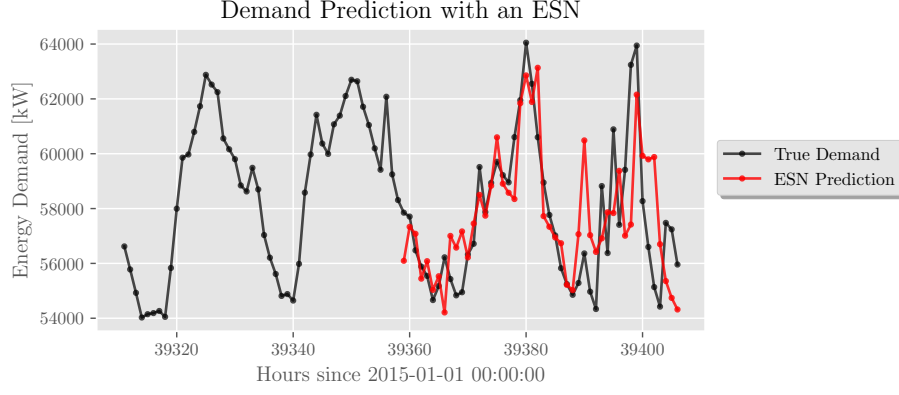
Figure 5: The optimized 4 hour ahead demand prediction. The training inputs for this forecast were historical hourly demand and solar elevation angle. *Hyperparameters*: Reservoir Size: 2500, Sparsity: 0.01, Spectral Radius: 1.5, Noise: 0.003, Training Length: 5000, Prediction Window: 4, Random state: 85.

Table 6: Tabulated error for 4-hour ahead electricity demand forecasts with various coupled quantities.

Scenario	NRMSE	MAE	RMSE	Improvement MAE (%)	Improvement RMSE (%)
Total Demand	0.83634	0.0193	0.0263	[-]	[-]
Demand + Sun Elevation	0.75855	0.0183	0.0239	-5.1831	-9.1255
Demand + Humidity	0.92245	0.0219	0.0290	+13.4715	+10.2662
Demand + Pressure	0.86714	0.0186	0.0273	-3.6269	+3.8023
Demand + Wet Bulb Temp.	0.80366	0.0196	0.0253	+1.5544	-3.8023
Demand + Dry Bulb Temp.	0.85662	0.0208	0.0270	+7.7720	+2.6616
Demand + Wind Speed	0.85152	0.0201	0.0268	+4.1451	+1.9011

3.3. ESN Forecasting: Solar Energy

We repeated the 4-hour and 48-hour ahead forecasts for solar energy production on the UIUC campus. Figure 6 and Figure 7 show the best forecasts for 48-hours ahead and 4-hours ahead, respectively. The shaded gray regions emphasize periods when the predicted energy production dipped below zero. This should never occur in reality. Table 7 shows that relative humidity was the

15

best additional feature for improving the 48-hour ahead prediction, while Table 8 shows that wet bulb temperature improved the forecast the most. In both cases, the predictions were improved by each feature, except for air pressure and wind speed.

₁₆₀   Our results are comparable to other work that used ESNs to forecast solar energy [30]. However, these results show that conventional ESNs are insufficient for improving energy economics through day-ahead forecasting [11].
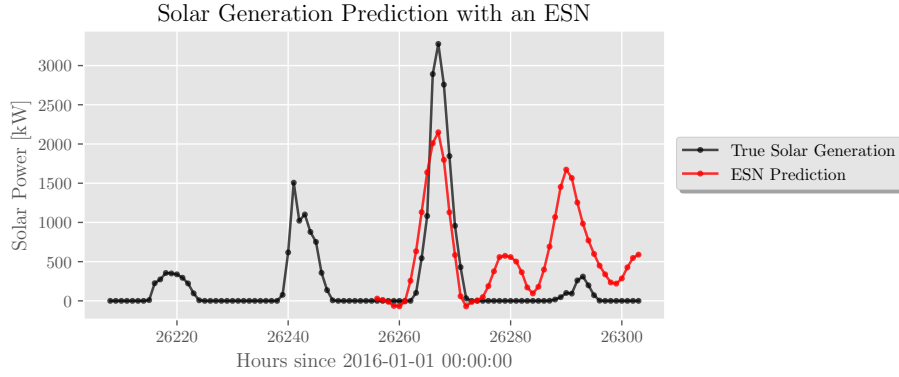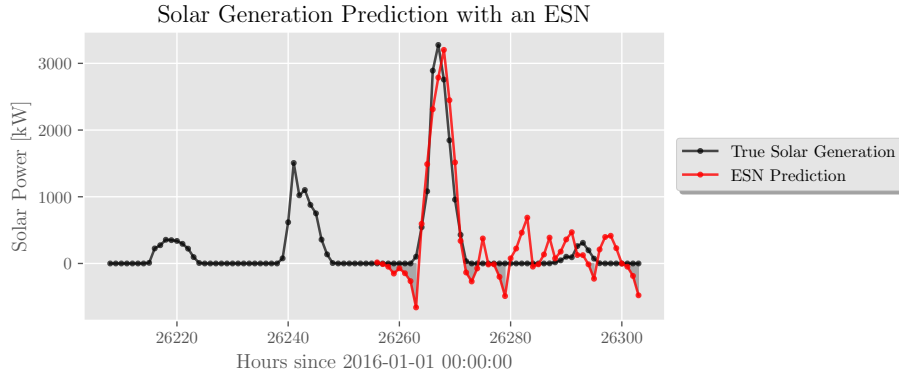

Figure 6: The optimized 48-hour ahead solar energy prediction. The training inputs for this forecast were historical solar energy and relative humidity. Hyperparameters: Reservoir Size: 800, Sparsity: 0.2, Spectral Radius: 1.5, Noise: 0.0001, Training Length: 5000, Prediction Window: 48, Random state: 85

Table 7: Tabulated error for 48-hour ahead solar energy forecasts with various coupled quantities.

Scenario	NRMSE	MAE	RMSE	Improvement MAE (%)	Improvement RMSE (%)
Solar Energy	1.27301	0.1433	0.2062	[-]	[-]
Solar + Sun Elevation	0.84908	0.0957	0.1375	-33.2170	-33.3172
Solar + Humidity	0.80107	0.1001	0.1297	-30.1465	-37.1000
Solar + Pressure	1.33226	0.1910	0.2158	+33.2868	+4.6557
Solar + Wet Bulb Temp.	1.16352	0.1519	0.1884	+6.0014	-8.6324
Solar + Dry Bulb Temp.	0.93376	0.1080	0.1512	-24.6336	-26.6731
Solar + Wind Speed	1.54306	0.2136	0.2500	+49.0579	+21.2415

Figure 7: The optimized 4 hour ahead solar energy prediction. The training inputs for this forecast were historical solar energy and hourly wet bulb temperature. *Hyperparameters*: Reservoir Size:800, Sparsity: 0.01, Spectral Radius: 0.9, Noise: 0.0001, Training Length: 5000, Prediction Window: 4, Random state: 85

3.4. ESN Forecasting: Wind Energy

Finally, we performed the same prediction tasks as before for wind energy. Figure 8 and Figure 9 show the best forecasts that minimized the RMSE for 48- and 4-hours ahead, respectively. All features except air pressure improved the forecast. Including solar elevation angle improved the 48-hour ahead forecast the most, while adding windspeed improved the 4-hour ahead forecast the most.

17

Table 8: Tabulated error for 4-hour ahead solar energy forecasts with various coupled quantities.

Scenario	NRMSE	MAE	RMSE	Improvement MAE (%)	Improvement RMSE (%)
Solar Energy	0.59151	0.0614	0.0958	[-]	[-]
Solar + Sun Elevation	0.51383	0.0554	0.0832	-9.7720	-13.1524
Solar + Humidity	0.59943	0.0663	0.0971	+7.9804	+1.3570
Solar + Pressure	0.77968	0.0925	0.1263	+50.6515	+31.8372
Solar + Wet Bulb Temp.	0.41541	0.0526	0.0673	-14.3322	-29.7954
Solar + Dry Bulb Temp.	0.61334	0.0682	0.0993	+11.0749	+3.6534
Solar + Wind Speed	0.70216	0.0723	0.1137	+17.7524	+18.6848

Those results are shown in Table 9 and 10 respectively. Lopéz et al. 2018 developed an advanced algorithm based on ESN by replacing the neurons in the reservoir with LSTM blocks [28]. Our conventional ESN achieved results comparable to the algorithm from Lopéz et al. 2018 by simply adding a single meteorological predictor. Chitsazan et al. 2017 [47] compared wind speed forecasting with a conventional ESN to an ESN with nonlinear readouts and achieved better results with the base model than we did [47]. However, this could be attributed to the fact that they used data with 10-minute resolution and 10-minute prediction steps. Unfortunately they did not include information about the hyper-parameters used for each prediction task.

Still, the state-of-the-art Weather Research and Forecasting model [48], a numerical weather prediction model, far outperforms our best results. Additionally, the 48-hour ahead forecast accuracy needs to be an order of magnitude lower than our model for meaningful economic benefit. Thus, conventional ESNs are currently insufficient for applications in grid planning [9].
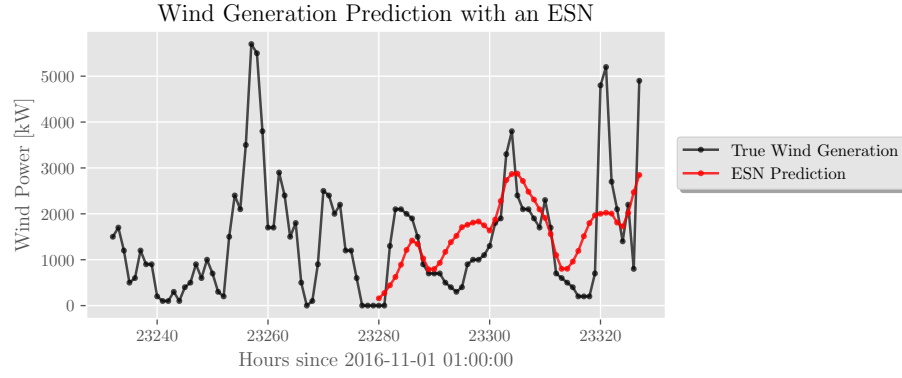
Figure 8: The optimized 48-hour ahead wind energy prediction that minimized the RMSE. The training inputs for this forecast were historical wind energy and solar elevation angle. *Hyperparameters*: Reservoir Size:1000, Sparsity: 0.1, Spectral Radius: 0.9, Noise: 0.0001, Training Length: 19100, Prediction Window: 48, Random state: 85

Table 9: Tabulated error for 48-hour ahead wind forecasts with various coupled quantities.

Scenario	NRMSE	MAE	RMSE	Improvement MAE (%)	Improvement RMSE (%)
Wind Energy	0.93167	0.1035	0.1308	[-]	[-]
Wind + Sun Elevation	0.81220	0.0857	0.1141	-17.1981	-12.7676
Wind + Humidity	0.84950	0.0952	0.1193	-8.0193	-8.7620
Wind + Pressure	0.98345	0.1076	0.1381	+3.9614	+5.5810
Wind + Wet Bulb Temp.	0.84323	0.0886	0.1184	-14.3961	-9.4801
Wind + Dry Bulb Temp.	0.86365	0.0815	0.1213	-21.2560	-7.2630
Wind + Wind Speed	0.84180	0.0763	0.1182	-26.2802	-9.6330

19
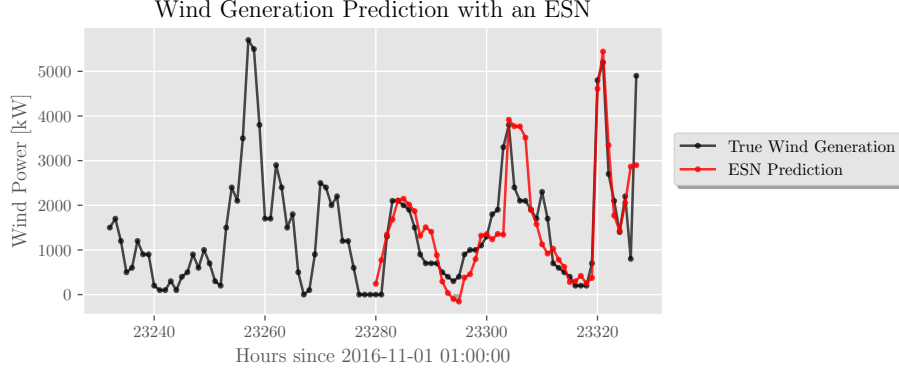
Figure 9: The optimized 4 hour ahead wind energy prediction. The training inputs for this forecast were historical wind energy and hourly windspeed. *Hyperparameters*: Reservoir Size:1000, Sparsity: 0.15, Spectral Radius: 0.9, Noise: 0.001, Training Length: 14300, Prediction Window: 4, Random state: 85

Table 10: Tabulated error for 4-hour ahead wind forecasts with various coupled quantities.

Scenario	NRMSE	MAE	RMSE	Improvement MAE (%)	Improvement RMSE (%)
Wind Energy	0.88507	0.0903	0.1243	[-]	[-]
Wind + Sun Elevation	0.83394	0.0705	0.1171	-21.9269	-5.7924
Wind + Humidity	0.85522	0.0813	0.1201	-9.9668	-3.3789
Wind + Pressure	0.88587	0.0866	0.1244	-4.0974	+0.0804
Wind + Wet Bulb Temp.	0.76203	0.0731	0.1070	-19.0476	-13.9179
Wind + Dry Bulb Temp.	0.79939	0.0747	0.1123	-17.2757	-9.9654
Wind + Wind Speed	0.59596	0.0571	0.0837	-36.7663	-32.6629

4. Discussion

¹⁸⁵ The forecast accuracy of our ESN for the Lorenz model does not persist for quite as long as in other work [31]. However, our model successfully replicates the environment that produces the Lorenz Attractor. Further, each randomly instantiated reservoir has a unique set of optimal hyper-parameters. It is impossible to replicate the exact conditions of other works without information

20

about a seed for the random state. We have included this information in Table 4 for future work to compare with our results.

For each target variable (demand, wind, and solar) we found that sun elevation angle, while not always the best, improved the forecast error in every case. We hypothesize that additional weather features effect model performance due to their temporal complexity relative to the target variable. Electricity demand, for example, is quite "predictable," and therefore has relatively low complexity. Meanwhile, air temperature and other weather related variables are less predictable. Thus, adding air temperature as a model input for electricity demand increases the total system complexity and weakens performance. Further, solar elevation angle is completely deterministic, perfectly predictable, and either improved, or neutrally effected, model performance in every case. Like electricity demand, solar elevation angle has both diurnal and annual periodicity but has lower complexity than air temperature and electricity demand itself. Conversely, solar and wind energy are both nonlinear functions of many weather variables and consequently have greater complexity than air temperature. Thus, adding temperature as a model input improved the forecast error because the total system complexity decreased relative to solar and wind energy alone. Including wind speed only improved the wind energy forecasts, likely because it has greater complexity than solar energy but less than wind energy. Relative humidity has an inconsistent and poorly understood effect on model performance. It improved the forecast for 48-hour ahead electricity demand but worsened it for the 4-hour ahead forecast, as shown in Table 5 and Table 6. The opposite trend occurred for solar energy. Quantifying the predictability and complexity of these systems is in progress.

These results point to an important disadvantage of using ESNs to forecast renewable energy: Although simple and fast, ESNs remain a black box. We assume that there exists some underlying dynamics in the energy system that can be "learned," but we cannot observe the learning process nor extract important features from ESNs.

We decided the forecast lengths based on the requirements for improved

economics and planning mentioned in the literature [9, 10, 11]. The ESN model performed reasonably well at predicting 4-hours ahead but did not improve on the state-of-the-art [9, 48]. The model did not perform well at the 48-hour ahead forecasts, potentially due to the lack of higher resolution data. ESNs are able to predict highly non-linear systems [49, 34], yet using hourly data could add spurious complexity that confounds the model [50]

4.1. Future Work

One appealing avenue of continued work is to leverage ESNs to generate synthetic data that respects real dynamics. Sythetic data are often useful for other machine learning or optimization algorithms. Typically, these data are produced by sampling from an Auto-Regressive Moving Average (ARMA) model [51, 52], which tacitly assumes the training data can be made stationary. ESNs can replicate the environment of a dynamical system, although it remains unclear how far in the future this behavior persists [31, 32]. Future work will also explore the effect of data resolution on model performance, as well as evaluate improvements to the ESN algorithm.

5. Conclusion

Improving renewable energy forecasting is important for grid-planning and unit commitment, especially as the share of variable renewable resources increases, challenging grid stability. We first demonstrated that our implementation of the ESN algorithm is consistent with the literature. Then, we used it to predict total demand, solar energy, and wind energy. Finally, we evaluated the influence of several meteorological factors on prediction accuracy. Our results show that researchers must carefully choose each additional training input to avoid increasing the system complexity. Our results also indicate that properly chosen training inputs can achieve comparable accuracy to more complex algorithms. The conventional ESN used here did not demonstrate an improvement over the state-of-the-art, nor was it accurate enough to improve grid-scale energy economy.

22

Future work will explore other applications of ESNs and pursue improvements
₂₅₀ to the model algorithm.

6. Acknowledgments

References

[1] The paris agreement | UNFCCC.
₂₆₅ URL `https://unfccc.int/process-and-meetings/`
`the-paris-agreement/the-paris-agreement`

[2] C. Cany, C. Mansilla, G. Mathonnière, P. da Costa, Nuclear contribution
to the penetration of variable renewable energy sources in a french decarbonised power mix 150 544–555. `doi:10.1016/j.energy.2018.02.122`.
₂₇₀ URL `http://www.sciencedirect.com/science/article/pii/`
`S0360544218303566`

[3] J. Chilvers, T. J. Foxon, S. Galloway, G. P. Hammond, D. Infield, M. Leach,
P. J. Pearson, N. Strachan, G. Strbac, M. Thomson, Realising transition
pathways for a more electric, low-carbon energy system in the united
₂₇₅ kingdom: Challenges, insights and opportunities 231 (6) 440–477, publisher:

23

IMECHE. `doi:10.1177/0957650917695448`.

URL `https://doi.org/10.1177/0957650917695448`

[4] 99th General Assembly, Illinois general assembly - full text of SB2814.

URL `http://www.ilga.gov/legislation/fulltext.asp?DocName=`
`&SessionId=88&GA=99&DocTypeId=SB&DocNum=2814&GAID=13&LegID=`
`96125&SpecSess=&Session=`

[5] iSEE, Illinois climate action plan (iCAP).

URL `https://sustainability.illinois.edu/`
`campus-sustainability/icap/`

[6] H. Haes Alhelou, M. E. Hamedani-Golshan, T. C. Njenda, P. Siano, A survey on power system blackout and cascading events: Research motivations and challenges 12 (4) 682, number: 4 Publisher: Multidisciplinary Digital Publishing Institute. `doi:10.3390/en12040682`.

URL `https://www.mdpi.com/1996-1073/12/4/682`

[7] J. H. Keppler, C. Marcantonini, O. N. E. Agency, O. for Economic Co-operation {and} Development, Carbon pricing, power markets and the competitiveness of nuclear power, Nuclear development, Nuclear Energy Agency, Organisation for Economic Co-operation and Development.

[8] Illinois Commerce Commision (ICC), I. P. A. (IPA), I. E. P. A. (IEPA), I. D. of Commerce and Economic Opportunity (IDCEO), Potential nuclear power plant closings in illinois.

URL `http://www.ilga.gov/reports/special/Report_Potential%`
`20Nuclear%20Power%20Plant%20Closings%20in%20IL.pdf`

[9] Q. Wang, C. B. Martinez-Anido, H. Wu, A. R. Florita, B.-M. Hodge, Quantifying the economic and grid reliability impacts of improved wind power forecasting 7 (4) 1525–1537, conference Name: IEEE Transactions on Sustainable Energy. `doi:10.1109/TSTE.2016.2560628`.

[10] E. V. Mc Garrigle, P. G. Leahy, Quantifying the value of improved wind energy forecasts in a pool-based electricity market 80 517–524. `doi:10.1016/j.renene.2015.02.023`.
URL `http://www.sciencedirect.com/science/article/pii/S0960148115001135`

[11] C. Brancucci Martinez-Anido, B. Botor, A. R. Florita, C. Draxl, S. Lu, H. F. Hamann, B.-M. Hodge, The value of day-ahead solar power forecasting improvement 129 192–203. `doi:10.1016/j.solener.2016.01.049`.
URL `http://www.sciencedirect.com/science/article/pii/S0038092X16000736`

[12] M. Lukoševičius, A practical guide to applying echo state networks, in: G. Montavon, G. B. Orr, K.-R. Müller (Eds.), Neural Networks: Tricks of the Trade: Second Edition, Lecture Notes in Computer Science, Springer, pp. 659–686. `doi:10.1007/978-3-642-35289-8_36`.
URL `https://doi.org/10.1007/978-3-642-35289-8_36`

[13] H. Liu, C. Chen, X. Lv, X. Wu, M. Liu, Deterministic wind energy forecasting: A review of intelligent predictors and auxiliary methods 195 328–345, publisher: Pergamon. `doi:10.1016/j.enconman.2019.05.020`.
URL `http://www.sciencedirect.com/science/article/pii/S0196890419305655`

[14] D. Lazos, A. B. Sproul, M. Kay, Optimisation of energy management in commercial buildings with weather forecasting inputs: A review 39 587–603. `doi:10.1016/j.rser.2014.07.053`.
URL `https://www.sciencedirect.com/science/article/pii/S136403211400505X`

[15] Y. Chen, H. Tan, U. Berardi, Day-ahead prediction of hourly electric demand in non-stationary operated commercial buildings: A clustering-based hybrid approach 148 228–237. `doi:10.1016/j.enbuild.2017.05.003`.

URL   https://www.sciencedirect.com/science/article/pii/
S0378778816313792

[16] I. Jayawardene, G. K. Venayagamoorthy, Comparison of echo state network and extreme learning machine for PV power prediction, in: 2014 IEEE Symposium on Computational Intelligence Applications in Smart Grid (CIASG), pp. 1–8, ISSN: 2326-7690. doi:10.1109/CIASG.2014.7011546.

[17] I. Jayawardene, G. Venayagamoorthy, Comparison of adaptive neuro-fuzzy inference systems and echo state networks for PV power prediction 53 92–102. doi:10.1016/j.procs.2015.07.283.

[18] G. Shi, D. Liu, Q. Wei, Energy consumption prediction of office buildings based on echo state networks 216 478–488. doi:10.1016/j.neucom.2016.08.004.
URL   http://www.sciencedirect.com/science/article/pii/
S0925231216308219

[19] M. A. Chitsazan, M. S. Fadali, A. Tryznadlowski, Wind speed and wind direction forecasting using echo state network with nonlinear functions 131 879–889, publisher: Pergamon. doi:10.1016/j.renene.2018.07.060.
URL   http://www.sciencedirect.com/science/article/pii/
S0960148118308577

[20] H. Hu, L. Wang, S.-X. Lv, Forecasting energy consumption and wind power generation using deep echo state network 154 598–613. doi:10.1016/j.renene.2020.03.042.
URL   http://www.sciencedirect.com/science/article/pii/
S0960148120303645

[21] A. Deihimi, H. Showkati, Application of echo state networks in short-term electric load forecasting 39 (1) 327–340. doi: 10.1016/j.energy.2012.01.007.
URL   https://linkinghub.elsevier.com/retrieve/pii/
S0360544212000126

[22] Y. Chen, Z. He, Z. Shang, C. Li, L. Li, M. Xu, A novel combined model based on echo state network for multi-step ahead wind speed forecasting: A case study of NREL 179 13–29. doi:10.1016/j.enconman.2018.10.068.
URL https://linkinghub.elsevier.com/retrieve/pii/S0196890418311968

[23] H. Wang, Z. Lei, Y. Liu, J. Peng, J. Liu, Echo state network based ensemble approach for wind power forecasting 201 112188. doi:10.1016/j.enconman.2019.112188.
URL http://www.sciencedirect.com/science/article/pii/S019689041931194X

[24] C. Gallicchio, A. Micheli, Deep echo state network (DeepESN): A brief surveyarXiv:1712.04323.
URL http://arxiv.org/abs/1712.04323

[25] X. Yao, Z. Wang, H. Zhang, A novel photovoltaic power forecasting model based on echo state network 325 182–189. doi:10.1016/j.neucom.2018.10.022.
URL http://www.sciencedirect.com/science/article/pii/S0925231218312104

[26] Q. Li, Z. Wu, R. Ling, L. Feng, K. Liu, Multi-reservoir echo state computing for solar irradiance prediction: A fast yet efficient deep learning approach 95 106481. doi:10.1016/j.asoc.2020.106481.
URL https://linkinghub.elsevier.com/retrieve/pii/S1568494620304208

[27] G. Holzmann, H. Hauser, Echo state networks with filter and a delay&sum readout.

[28] E. López, C. Valle, H. Allende, E. Gil, H. Madsen, Wind power forecasting based on echo state networks and long short-term memory 11 (3) 526, number: 3 Publisher: Multidisciplinary Digital Publishing Institute. doi:

27

10.3390/en11030526.

URL https://www.mdpi.com/1996-1073/11/3/526

[29] N. Chouikhi, B. Ammar, N. Rokbani, A. M. Alimi, PSO-based analysis
of echo state network parameters for time series forecasting 55 211–225.
doi:10.1016/j.asoc.2017.01.049.

URL https://linkinghub.elsevier.com/retrieve/pii/
S1568494617300649

[30] Q. Li, Z. Wu, R. Ling, M. Tan, Echo state network-based spatio-temporal
model for solar irradiance estimation 158 3808–3813, publisher: Elsevier.
doi:10.1016/j.egypro.2019.01.868.

URL http://www.sciencedirect.com/science/article/pii/
S1876610219309105

[31] J. Pathak, Z. Lu, B. R. Hunt, M. Girvan, E. Ott, Using machine learning
to replicate chaotic attractors and calculate lyapunov exponents from data
27 (12) 121102. arXiv:1710.07313, doi:10.1063/1.5010300.

URL http://arxiv.org/abs/1710.07313

[32] J. Pathak, B. Hunt, M. Girvan, Z. Lu, E. Ott, Model-free prediction of
large spatiotemporally chaotic systems from data: A reservoir computing
approach 120 (2) 024102, publisher: American Physical Society. doi:
10.1103/PhysRevLett.120.024102.

URL https://link.aps.org/doi/10.1103/PhysRevLett.120.024102

[33] P. R. Vlachas, J. Pathak, B. R. Hunt, T. P. Sapsis, M. Girvan, E. Ott,
P. Koumoutsakos, Backpropagation algorithms and reservoir computing in
recurrent neural networks for the forecasting of complex spatiotemporal
dynamics 126 191–217. doi:10.1016/j.neunet.2020.02.016.

URL http://www.sciencedirect.com/science/article/pii/
S0893608020300708

[34] M. Lukoševičius, H. Jaeger, Reservoir computing approaches
to recurrent neural network training 3 (3) 127–149. doi:

10.1016/j.cosrev.2009.03.005.

URL http://www.sciencedirect.com/science/article/pii/S1574013709000173

420 [35] C. Korndörfer, pyESN.

URL https://github.com/cknd/pyESN

[36] E. N. Lorenz, Deterministic nonperiodic flow 20 (2) 130–141, publisher: American Meteorological Society Section: Journal of the Atmospheric Sciences. doi:10.1175/1520-0469(1963)020<0130:DNF>2.0.CO;2.

425 URL https://journals.ametsoc.org/view/journals/atsc/20/2/1520-0469_1963_020_0130_dnf_2_0_co_2.xml

[37] AlsoEnergy, University of illinois solar farm dashboard, http://go.illinois.edu/solar.

URL http://go.illinois.edu/solar

430 [38] M. Marquissee, Campus electricity demand and wind PowerData.

[39] N. C. for Environmental Information, Find a station | data tools | climate data online (CDO) | national climatic data center (NCDC).

URL https://www.ncdc.noaa.gov/cdo-web/datatools/findstation

[40] S. Breitweiser, Wind power: University of illinois at urbana-champaign.

435 URL https://www.fs.illinois.edu/docs/default-source/news-docs/newsrelease_windppa___factsheet.pdf?sfvrsn=43aaffea_0

[41] National solar radiation data base - NSRDB viewer - OpenEI datasets.

URL https://openei.org/datasets/dataset/

440 national-solar-radiation-data-base/resource/b2074dd9-36a4-4382-a12f-e795b578404c

[42] H. E. Garcia, J. Chen, J. S. Kim, M. G. McKellar, W. R. Deason, R. B. Vilim, S. M. Bragg-Sitton, R. D. Boardman, Nuclear hybrid

29

energy systems regional studies: West texas & northeastern arizona. doi:10.2172/1236837.

URL https://www.osti.gov/biblio/1236837-nuclear-hybrid-energy-systems-regional-studies-

[43] N. US Department of Commerce, ESRL global monitoring laboratory - global radiation and aerosols.

URL https://www.esrl.noaa.gov/gmd/grad/solcalc/calcdetails. html

[44] J. Meeus, Astronomical Algorithms, 2nd Edition, Willmann-Bell, Inc.

[45] P. Kobylinski, M. Wierzbowski, K. Piotrowski, High-resolution net load forecasting for micro-neighbourhoods with high penetration of renewable energy sources 117 105635. doi:10.1016/j.ijepes.2019.105635.

URL http://www.sciencedirect.com/science/article/pii/ S0142061518335257

[46] D. L. Marino, K. Amarasinghe, M. Manic, Building energy load forecasting using deep neural networks, in: IECON 2016 - 42nd Annual Conference of the IEEE Industrial Electronics Society, pp. 7046–7051. doi:10.1109/ IECON.2016.7793413.

[47] M. A. Chitsazan, M. S. Fadali, A. K. Nelson, A. M. Trzynadlowski, Wind speed forecasting using an echo state network with nonlinear output functions, in: 2017 American Control Conference (ACC), pp. 5306–5311, ISSN: 2378-5861. doi:10.23919/ACC.2017.7963779.

[48] J. G. Powers, J. B. Klemp, W. C. Skamarock, C. A. Davis, J. Dudhia, D. O. Gill, J. L. Coen, D. J. Gochis, R. Ahmadov, S. E. Peckham, G. A. Grell, J. Michalakes, S. Trahan, S. G. Benjamin, C. R. Alexander, G. J. Dimego, W. Wang, C. S. Schwartz, G. S. Romine, Z. Liu, C. Snyder, F. Chen, M. J. Barlage, W. Yu, M. G. Duda, The weather research and forecasting model: Overview, system efforts, and future directions 98 (8) 1717–1737, publisher: American Meteorological Society Section: Bulletin of

the American Meteorological Society. `doi:10.1175/BAMS-D-15-00308.1`.
URL `https://journals.ametsoc.org/view/journals/bams/98/8/bams-d-15-00308.1.xml`

[49] H. Jaeger, Harnessing nonlinearity: Predicting chaotic systems and saving energy in wireless communication 304 (5667) 78–80. `doi:10.1126/science.1091277`.
URL `https://www.sciencemag.org/lookup/doi/10.1126/science.1091277`

[50] J. Garland, R. James, E. Bradley, Model-free quantification of time-series predictability 90 (5) 052910, publisher: American Physical Society. `doi:10.1103/PhysRevE.90.052910`.
URL `https://link.aps.org/doi/10.1103/PhysRevE.90.052910`

[51] T. E. Baker, A. S. Epiney, C. Rabiti, E. Shittu, Optimal sizing of flexible nuclear hybrid energy system components considering wind volatility 212 498–508.

[52] H. E. Garcia, J. Chen, J. S. Kim, R. B. Vilim, W. R. Binder, S. M. Bragg Sitton, R. D. Boardman, M. G. McKellar, C. J. J. Paredis, Dynamic performance analysis of two regional nuclear hybrid energy systems 107 234–258. `doi:10.1016/j.energy.2016.03.128`.
URL `http://www.sciencedirect.com/science/article/pii/S0360544216303759`